

Dr. Oglione. This is fantastic! We have 70 000 meteorites but many fewer 'fresh' meteorites from witnessed falls. The more we collect the higher the chance we're going to get something that is really amazing, like something on a hyperbolic orbit or from the Kuiper Belt.

The President. I often wonder about doing spectroscopic analysis on those. It won't tell you about isotopes but it will give you chemistry. I think we should thank all three speakers [applause]. You are all invited, as usual, for drinks across the road in our new premises and the next meeting will be Friday, January 10th.

REDISCUSSION OF ECLIPSING BINARIES. PAPER 24:
THE δ SCUTI PULSATOR V596 PUP (FORMERLY KNOWN AS VV PYX)

By *John Southworth*

Astrophysics Group, Keele University

V596 Pup is a detached eclipsing binary containing two A1V stars in a 4.596-d-period orbit with a small eccentricity and apsidal motion, previously designated as VV Pyxidis. We use new light-curves from the *Transiting Exoplanet Survey Satellite (TESS)* and published radial velocities to determine the physical properties of the component stars. We find masses of $2.098 \pm 0.021 M_{\odot}$ and $2.091 \pm 0.018 M_{\odot}$, and radii of $2.179 \pm 0.008 R_{\odot}$ and $2.139 \pm 0.007 R_{\odot}$. The measured distance to the system is affected by the light from a nearby companion star; we obtain 178.4 ± 2.5 pc. The properties of the system are best matched by theoretical predictions for a subsolar metallicity of $Z = 0.010$ and an age of 570 Myr. We measure seven significant pulsation frequencies from the light-curve, six of which are consistent with δ Scuti pulsations and one of which is likely of slowly-pulsating B-star type.

Introduction

Eclipsing binary systems contain the only stars for which a direct measurement of their mass and radius is possible. Detached eclipsing binaries (dEBs) are an important class of these objects because their components have evolved as single stars. Their measured properties can be compared to the predictions of theoretical models of stellar evolution to check the reliability of the predictions and help calibrate the physical ingredients of the models¹⁻³.

Another approach to improving the theoretical descriptions of stars is that of asteroseismology⁴. The measured stellar oscillation frequencies can be compared to theoretical predictions to infer their densities, ages, rotational profiles, and the strength of chemical mixing⁵⁻⁸.

Some dEBs show the signs of pulsations in one or both components, and thus might provide more exacting constraints on stellar theory. The pulsational types so far found in dEBs include δ Scuti^{9–12}, γ Doradus^{13,14}, slowly-pulsating B-type (SPB)^{15,16}, and β Cephei^{17–19}. Several of these have been studied in previous papers in the current series: the hybrid δ Sct/ γ Dor systems RR Lyn²⁰ and GK Dra²¹, and the high-mass pulsators V1388 Ori²² and V1765 Cyg²³.

In this work we present an analysis of V596 Puppis (Table I) based on published spectroscopy and new space-based photometry. We include an independent discovery of δ Scuti pulsations in this object.

V596 Puppis

The variability of V596 Pup was discovered from photographic patrol plates by Strohmeier, Knigge & Ott³² without further comment. Andersen & Nordström³³ found it to exhibit double lines which were sharp and underwent large-radial velocity (RV) variations. Olsen³⁴ obtained 67 photoelectric brightness measurements which showed it to have two sets of eclipses with approximately equal depth. The secondary eclipse occurred at phase 0.48, indicating an eccentric orbit. It was given the name VV Pyx in the *65th Name-list of variable stars*³⁵.

The only detailed analysis of V596 Pup is by Andersen, Clausen & Nordström³¹ (hereafter ACN84), who obtained complete light-curves (1495 points³⁶ in each of the *uvby* passbands) using the Strömrgren photometer³⁷ on the Copenhagen 50-cm telescope at ESO La Silla, Chile, and photographic spectroscopy (28 high-dispersion photographic plates, each yielding an RV measurement for both stars). They confirmed the orbital eccentricity, detected apsidal motion, measured a spectral-line-strength ratio of 1.00 ± 0.03 between the stars, and found projected rotational velocities of $v \sin i = 23 \pm 3$ km s⁻¹ for both stars. Due to the similarity of the two stars, ACN84 assumed they were identical and presented the physical properties of the mean component of the system. A *V*-band light-curve has since been presented by Shobbrook³⁸.

Samus *et al.*³⁹ performed a comprehensive revision of the sky positions of objects included in the *General Catalogue of Variable Stars (GCVS*)*. In 38 cases the variables were found to be in a different constellation than that adopted for their original *GCVS* designation, either due to changes in constellation boundaries, proper motion, or improved measurement of their right ascension and declination. Kazarovets *et al.*⁴⁰ specified new names for these 38 variable stars, at which point our object of interest became V596 Pup instead of VV Pyx.

V596 Pup has a close visual companion which is moderately fainter. The *Index Catalogue of Visual Double Stars*⁴¹ gives a separation of 0.3 arcsec and a brightness difference of 1.1 mag. Jens Viggo Clausen obtained a visual estimate of the magnitude difference of 2 mag on a night of good seeing, which is in good agreement with spectroscopic measurements from two deep photographic plates (ACN84). ACN84 further suggested that the companion shows RV variability so could itself be a binary system. McAlister *et al.*^{42,43} found angular separations of 0.397 arcsec and 0.417 arcsec, respectively, *via* speckle interferometry; further measurements were made by this group but are not itemized here. The *Gaia* DR3 entry of V596 Pup (Table I) gives an unusually imprecise parallax (4.31 ± 0.17 mas) and a large RUWE (renormalized unit-weight error) of 4.8, suggesting the positional measurements were compromised by the nearby companion. The RUWE should be approximately 1.0, and a value above 1.4 is

* <http://www.sai.msu.su/gcvs/gcvs/>

TABLE I

Basic information on V596 Puppis. The BV magnitudes are each the mean of 87 individual measurements²⁴ distributed approximately randomly in orbital phase. The JHK_s magnitudes are from 2MASS²⁵ and were obtained at orbital phase 0.673.

Property	Value	Reference
Right ascension (J2000)	08 ^h 27 ^m 33 ^s .275	26
Declination (J2000)	−20°50′38″.25	26
Bright Star Catalogue	HR 3335	27
Henry Draper designation	HD 71581	28
Gaia DR3 designation	5706279565053294848	29
Gaia DR3 parallax	4.3083 ± 0.1673 mas	29
TESS Input Catalog designation	TIC 144085463	30
B magnitude	6.63 ± 0.01	24
V magnitude	6.59 ± 0.01	24
J magnitude	6.403 ± 0.018	25
H magnitude	6.410 ± 0.024	25
K _s magnitude	6.374 ± 0.024	25
Spectral type	A1 V + A1 V	31

indicative of a poor astrometric solution²⁹; lower boundaries of 1.2 to 1.3 have been given by other authors^{44,45}.

ACN84 found an apsidal period of $U = 3200^{+1400}_{-800}$ yr. The relativistic contribution to this is significant, and it was identified by Giménez⁴⁶ as a candidate for the detection of this phenomenon. The apsidal motion of the system has subsequently been discussed by many authors^{47–50}. The most recent work, by Claret *et al.*⁵¹, found a significantly shorter apsidal period of 758 ± 29 yr.

Finally, Kahraman Aliçavuş *et al.*⁵² included V596 Pup in a list of 42 eclipsing systems which show pulsations. A set of peaks in the frequency spectrum of the system in the region of 35–40 d^{−1} were interpreted as resulting from δ Scuti pulsations.

Photometric observations

V596 Pup has been observed in three sectors by the NASA *Transiting Exoplanet Survey Satellite*⁵³ (TESS). The data from sector 8 were obtained at a cadence of 1800 s, and from sectors 34 and 61 at a cadence of 120 s. Our analysis below concentrates on the data at 120-s cadence to avoid the smearing effects of the longer cadence. A fourth set of TESS observations (sector 88) was obtained in 2025 January but was not available when our analysis began.

The data were downloaded from the NASA Mikulski Archive for Space Telescopes (MAST*) using the LIGHTKURVE package⁵⁴. We specified the quality flag “hard” to reject low-quality data, and used the simple aperture photometry (SAP) light-curves from the SPOC data-reduction pipeline⁵⁵. The data from sector 8 were only available in QLP (Quick-Look Pipeline) form⁵⁶ and were also obtained using LIGHTKURVE. We converted the data points into differential magnitudes and subtracted the median magnitude from each sector for normalization. The light-curves are shown in Fig. 1 and contain 747, 17373, and 17764 data points from sectors 8, 34, and 61, respectively.

Light-curve analysis

The eclipses in V596 Pup occupy 14% of each orbital period, and the remaining data hold little information about the properties of the system.

*<https://mast.stsci.edu/portal/Mashup/Clients/Mast/Portal.html>

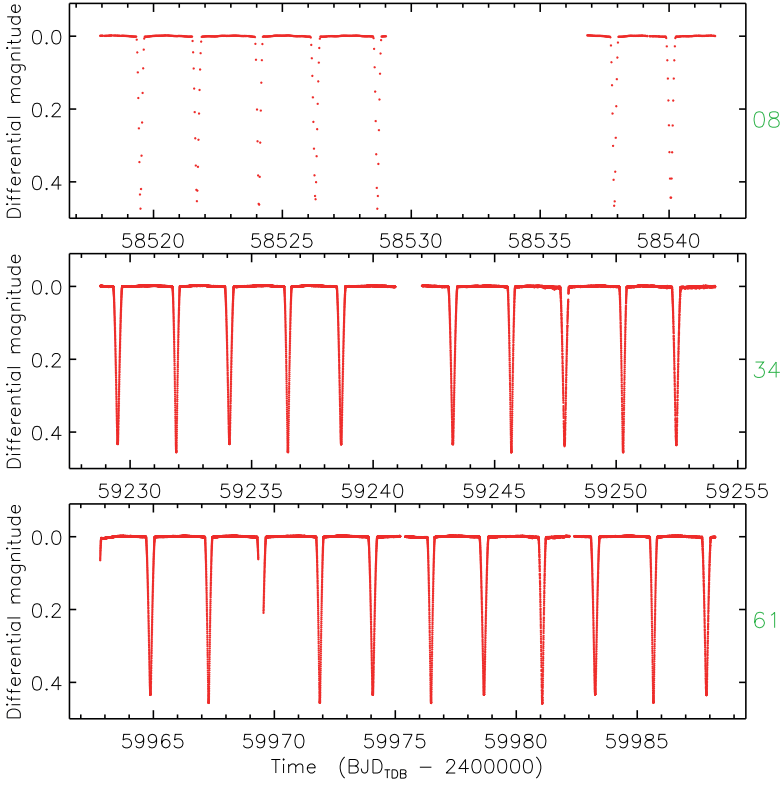


FIG. 1

TESS photometry of V596 Pup. The flux measurements have been converted to magnitude units then rectified to zero magnitude by subtraction of the median. The data from sector 8 are from the QLP pipeline, and from sectors 34 and 61 from the SPOC pipeline. The sector number is shown in green to the right of each panel.

We therefore extracted the data around each eclipse from the short-cadence light-curves by retaining only the data points within one full eclipse duration of the midpoint of a fully-observed eclipse. This left a total of 4826 data points from sector 34, and 4753 from sector 61. We define star A to be eclipsed at the deeper eclipse, and its companion to be star B.

We modelled the light-curves of the eclipses using version 43 of the JKTEBOP* code^{57,58}. The fitted parameters were the fractional radii of the stars (r_A and r_B), expressed as their sum ($r_A + r_B$) and ratio ($k = r_B/r_A$), the central-surface-brightness ratio (\mathcal{F}), third light (L_3), orbital inclination (i), orbital period (P), the reference time of primary minimum (T_0), and the quantities $e \cos \omega$ and $e \sin \omega$ where e is the orbital eccentricity and ω is the argument of periastron. Limb darkening (LD) was accounted for using the power-2 law⁵⁹⁻⁶¹ with the same LD coefficients for both stars due to their similarity. The linear coefficient (c) was

*<http://www.astro.keele.ac.uk/jkt/codes/jktebop.html>

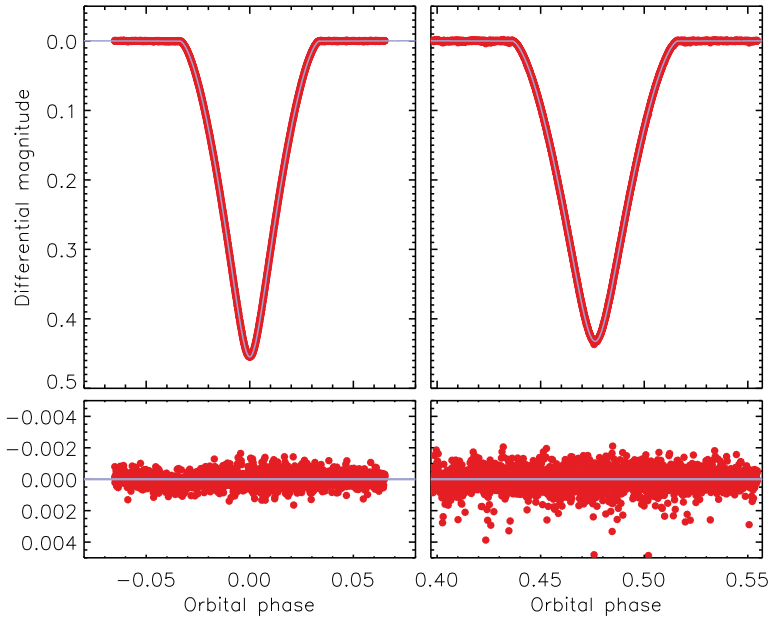


FIG. 2

JKTEBOP best fit to the light-curves of V596 Pup from *TESS* sector 34. The data are shown as filled red circles and the best fit as a light blue solid line. The residuals are shown on an enlarged scale in the lower panel.

fitted and the non-linear coefficient (α) held fixed at a theoretical value^{62,63}. Our initial fits to sectors 34 and 61 together led to a larger scatter than expected. We further constrained the ephemeris by measuring a time of primary eclipse from sector 8 and including it in the fit, finding that this made things worse (the best-fitting time of minimum from sector 8 was 29σ from the measured value). From this we deduce that the effects of apsidal motion are significant over the time interval of the *TESS* observations, and also that the amount of third light may differ between sectors due to the different orientations of the *TESS* cameras. A natural solution is to model the data from sectors 34 and 61 individually, and leave discussion of the apsidal motion to future work. This resulted in much better fits being obtained, which are shown in Figs. 2 and 3. The best-fitting parameter values are given in Table II. The residuals *versus* the best fits are larger in the secondary eclipse than in the primary eclipse, for both sectors. Inspection of the residuals *versus* time suggests that this is due to chance. We experimented with rejecting the eclipses with higher scatter but found that this had little effect on the results.

The parameter uncertainties were obtained using Monte-Carlo (MC) and residual-permutation (RP) simulations (JKTEBOP tasks 8 and 9). As part of this process the data errors from the *TESS* reduction pipeline were normalized to force a reduced χ^2 of unity. We were expecting the RP error bars to be larger than the MC ones due to the pulsational signatures in the light-curve, which were not included in the model and thus are effectively red noise, but for most

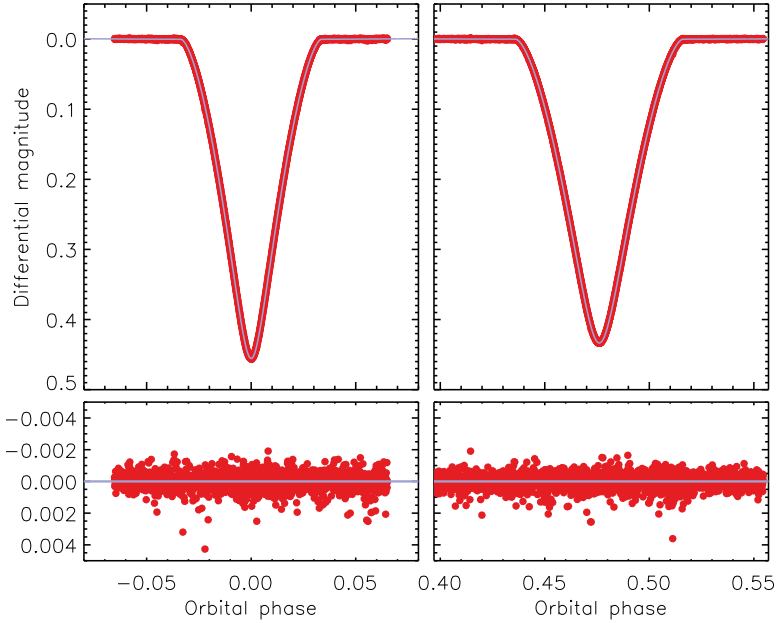


FIG. 3

JKTEBOP best fit to the light-curves of V596 Pup from *TESS* sector 61. Other comments are the same as for Fig. 2.

parameters the two were very similar. The main exception to this is $e \cos \omega$, from which we infer that the pulsations affect the measured phase difference between the eclipses.

Table II contains the measured parameters from the fits to sectors 34 and 61, plus the larger of the MC or RP error bar for each parameter. Given the similarity of the data and results for the two sectors we adopt the unweighted mean of those values in common. The uncertainties are extremely low so we take the largest of the four options for each parameter (Table II), thus forego the $\sqrt{2}$ boost from having two datasets fitted separately.

The analysis above provides measurements of the fractional radii of the stars to a precision of 0.15%. The surface-brightness ratio is almost unity: the difference in the depths of primary and secondary eclipse is driven primarily by different fractions of the stars eclipsed at these times due to the eccentricity of the orbit. Two orbital ephemerides are also obtained, but are not valid for other time periods as they don't account for the apsidal motion.

Radial-velocity analysis

Armed with a new high-precision measurement of the orbital eccentricity, it was reasonable to reanalyse the published RVs of the stars (ACN84) to see if they were consistent and allowed a more precise measurement of the velocity amplitudes, K_A and K_B . We manually digitized the RVs in table 2 of ACN84 then fitted spectroscopic orbits (see below). We found that the RVs for both

TABLE II
Photometric parameters of V596 Pup measured using KTEBOP from the light-curves from TESS sectors 34 and 61. The error bars are 1 σ and were obtained from a residual-permutation analysis.

Parameter	Value (sector 34)	Value (sector 61)	Adopted value
<i>Fitted parameters:</i>			
Orbital period (d)	4.5961598 ± 0.0000025	4.5961597 ± 0.0000023	88.1340 ± 0.0055
Reference time (BJD _{TDB})	2459236.4944615 ± 0.0000066	2459976.4770916 ± 0.0000049	0.23022 ± 0.00012
Orbital inclination (°)	88.1294 ± 0.0055	88.1387 ± 0.0038	0.9817 ± 0.0027
Sum of the fractional radii	0.23018 ± 0.00012	0.23027 ± 0.00011	0.99925 ± 0.00035
Ratio of the radii	0.9820 ± 0.0027	0.9815 ± 0.0021	
Central-surface-brightness ratio	0.99906 ± 0.00035	0.99944 ± 0.00027	
Third light	0.2026 ± 0.0010	0.1999 ± 0.0010	
LD coefficient c	0.554 ± 0.015	0.560 ± 0.011	0.557 ± 0.015
LD coefficient α	0.4574 (fixed)	0.4574 (fixed)	0.4574 (fixed)
$e \cos \omega$	-0.0370930 ± 0.0000089	-0.0374236 ± 0.0000064	
$e \sin \omega$	0.08941 ± 0.00021	0.08963 ± 0.00016	
<i>Derived parameters:</i>			
Fractional radius of star A	0.11614 ± 0.00017	0.11621 ± 0.00013	0.11617 ± 0.00017
Fractional radius of star B	0.11404 ± 0.00016	0.11406 ± 0.00013	0.11405 ± 0.00016
Light ratio f_B/f_A	0.9631 ± 0.0051	0.9626 ± 0.0040	0.9629 ± 0.0051
Orbital eccentricity	0.09680 ± 0.00019	0.09713 ± 0.00015	0.09696 ± 0.00019
Argument of periastron (°)	112.533 ± 0.048	112.663 ± 0.039	

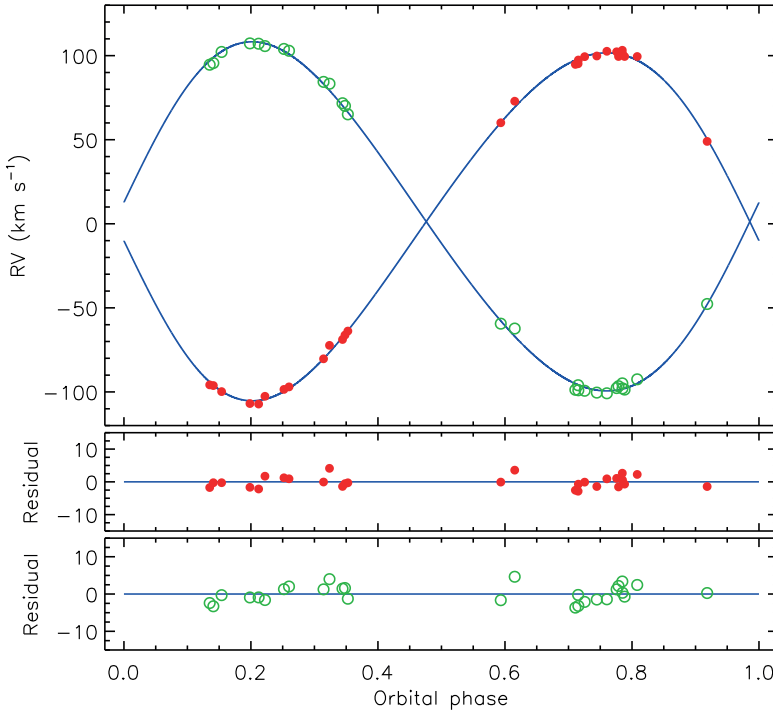


FIG. 4

RVs of V596 Pup from ACN84 compared to the best fit from JKTEBOP (solid blue lines). The RVs for star A are shown with red filled circles, and for star B with green open circles. The residuals are given in the lower panels separately for the two components.

stars at time HJD 2444348.5342 were highly discrepant, and that the time did not match the orbital phase in column 3 of the table. Changing the time to 2444384.5342 solved all three problems, and is more in line with the typical observing-run time allocations*.

We then fitted the RVs for the two stars using JKTEBOP. The only fitted parameters were K_A , K_B , ω , the systemic velocities of the stars, and a phase offset *versus* our orbital ephemeris from *TESS* sector 34. The phase offset is small (-0.011), so our star identifications match those of ACN84. The systemic velocities of the stars were very similar so we ran a final fit with a value common to both stars. Error bars were obtained from 1000 MC simulations⁶⁴. The measured parameters are $K_A = 103.47 \pm 0.37$ km s⁻¹, $K_B = 103.82 \pm 0.49$ km s⁻¹, $\omega = 108.0^\circ \pm 2.0^\circ$ and a systemic velocity of 1.31 ± 0.26 km s⁻¹ (where the error bar does not include uncertainty in the definition of the velocity scale). The fitted orbits are shown in Fig. 4. The values and uncertainties we find are in good agreement with those from ACN84.

*The times of the RVs are grouped into three discrete observing runs of 5–10 days each.

Physical properties and distance to V596 Pup

We calculated the physical properties of V596 Pup using the JK TABSDIM code⁶⁶ with the P , e , i , r_A , and r_B from our analysis of the *TESS* light-curves, and the K_A and K_B from our analysis of the ACN84 RVs. We adopted an effective temperature of $T_{\text{eff}} = 8500 \pm 200$ K from ACN84 for both stars, as their surface brightnesses are practically identical. A somewhat larger value of 9311 ± 195 K was given by Zorec & Royer⁶⁷.

Our mass and radius measurements (Table III) are consistent with those of ACN84, with the advantages that we have values for both stars rather than just the mean component, and that the radii are now measured to a precision of 0.3% versus 0.9%. The synchronous rotation velocities in Table III are consistent with the measured values (ACN84).

The distance to V596 Pup merits discussion. Inversion of the parallax from the *Hipparcos* and *Gaia* satellites give distances of 222^{+63}_{-40} pc and 232 ± 9 pc, respectively. However, the *Gaia* value is unusually uncertain for a celestial object this close to the Solar System, and is accompanied by a RUWE indicating a poor astrometric fit (see *Introduction*). ACN84 determined a distance of 195 ± 10 pc, somewhat shorter than both parallax-derived values (albeit that the *Hipparcos* distance is very uncertain).

We calculated a new distance estimate using the BV and \mathcal{JHK}_s apparent magnitudes of the system (Table I), the calibrations of surface brightness versus T_{eff} presented by Kervella *et al.*⁶⁸, and the other quantities inputted to JK TABSDIM. The \mathcal{JHK}_s magnitudes were converted to the Johnson system⁶⁹ but not corrected for the presence of the close companion. With an interstellar reddening of $E(B-V) = 0.07 \pm 0.02$ mag to equalize the distances at optical and infrared wavelengths, we obtained a much shorter distance of 162.8 ± 2.2 pc in the K_s band. An alternative approach using theoretical bolometric corrections from Girardi *et al.*⁷⁰ gives a consistent distance of 165.1 ± 2.3 pc.

The star within 0.4 arcsec of V596 Pup will contaminate the photometry of the system. Without a precise magnitude difference and T_{eff} of the star we cannot properly correct for its contamination in the BV and \mathcal{JHK}_s magnitudes. Its light acts to make V596 Pup appear brighter and therefore closer to the observer. If we adopt a magnitude difference of 1.1 mag in all passbands⁴¹ we find a distance of 190.1 pc instead of 162.8 pc; for a magnitude difference of 2 mag (ACN84) the distance becomes 175.3 pc. Our preferred option is instead

TABLE III

Physical properties of V596 Pup defined using the nominal solar units given by IAU 2015 Resolution B3 (ref. 65).

Parameter	Star A	Star B
Mass ratio M_B/M_A	0.9966 \pm 0.0059	
Semi-major axis of relative orbit (R_\odot^N)	12.109 \pm 0.029	
Mass (M_\odot^N)	2.098 \pm 0.021	2.091 \pm 0.018
Radius (R_\odot^N)	2.1785 \pm 0.0072	2.1387 \pm 0.0070
Surface gravity (log[cgs])	4.0835 \pm 0.0024	4.0981 \pm 0.0020
Density (ρ_\odot)	0.2029 \pm 0.0011	0.2137 \pm 0.0011
Synchronous rotational velocity (km s ⁻¹)	23.98 \pm 0.08	23.54 \pm 0.08
Effective temperature (K)	9500 \pm 200	9500 \pm 200
Luminosity log(L/L_\odot^N)	1.542 \pm 0.037	1.526 \pm 0.037
M_{bol} (mag)	0.885 \pm 0.092	0.925 \pm 0.092
Interstellar reddening $E(B-V)$ (mag)	0.07 \pm 0.02	
Distance (pc)	178.4 \pm 2.5	

to interpret the third light in our solutions of the *TESS* light-curves as arising from the nearby star. In this case the amount of contamination is at least precisely determined, and we obtain a distance of 178.4 pc with a negligible additional uncertainty.

We cannot find a way to make our distance match that from *Gaia* DR3. Ignoring interstellar extinction changes the K_s -band distance by only +2.7 pc. Adding 1000 K to the T_{eff} values requires a larger $E(B-V)$ and only shifts the distance measurement by +2.4 pc. Such a small effect might seem surprising, but is explicable: our preferred distance estimates rely primarily on the K_s band, which is well into the Rayleigh-Jeans tail of the spectrum so is insensitive to temperature. The 2MASS JHK_s apparent magnitudes were taken at orbital phase 0.673 so are well away from eclipse — if they were in eclipse then this would make them fainter and bring the measured distance even closer. We conclude that the *Hipparcos* parallax is too uncertain to conflict with our results, that the *Gaia* DR3 parallax is unreliable due to the close companion, and that our own distance measurements are also imperfect as they incorporate assumptions about the brightness and T_{eff} of the close companion.

Comparison with theoretical models

The similarity of the components of V596 Pup means the system is not a particularly good test of theoretical models, but a comparison is still informative. We compared the measured properties of V596 Pup to the predictions of the PARSEC 1.2S theoretical stellar-evolutionary models⁷², concentrating on the radii and T_{eff} values predicted for the known masses.

A metal abundance of $Z = 0.017$ and an age of 540 Myr fits the radii well but underpredicts the T_{eff} values by 600 K. A lower metal abundance of $Z = 0.014$ requires an age of 560 Myr to match the radii but still underpredicts the T_{eff} values, by 400 K. Moving to a Z of 0.010 and an age of 570 ± 20 Myr provides an excellent match to all three properties for both stars. This suggests that V596 Pup is moderately metal-poor, something that should be confirmed spectroscopically. A Hertzsprung–Russell diagram is shown in Fig. 5.

Pulsation analysis

The *TESS* light-curve of V596 Pup shows clear evidence for pulsations of relatively short period. The object has been previously identified as showing δ Scuti pulsations⁵². We calculated frequency spectra for sectors 34 and 61 using version 1.2.0 of the PERIOD04 code⁷³. The sectors were treated individually to avoid problems with aliasing, and the JKTEBOP best fit was subtracted from the data prior to analysis. The frequency spectrum for sector 61 had a lower noise level so we used it to measure the significant frequencies in the light-curve.

We found seven significant frequencies in the spectrum for sector 61, where we take the minimum signal-to-noise ratio (S/N) to be 4 (refs. 74 and 75). All of these are also present in the spectrum for sector 34, confirming their existence. An additional frequency at 36.3 d^{-1} is present in sector 61 but not sector 34 so may not be of astrophysical origin. The frequencies and their amplitudes are given in Table IV, and the spectra are shown in Fig. 6.

Six of the frequencies are in the interval $30\text{--}50 \text{ d}^{-1}$ so can be attributed to pulsations of the δ Scuti type. The T_{eff} and luminosity values of the stars put them slightly beyond the instability strip and in a region where the fraction of pulsators is approximately 0.1 (see Murphy *et al.*⁷⁶). The remaining frequency is much lower, at 1.9 d^{-1} , and cannot be due to p-mode pulsations. It is instead

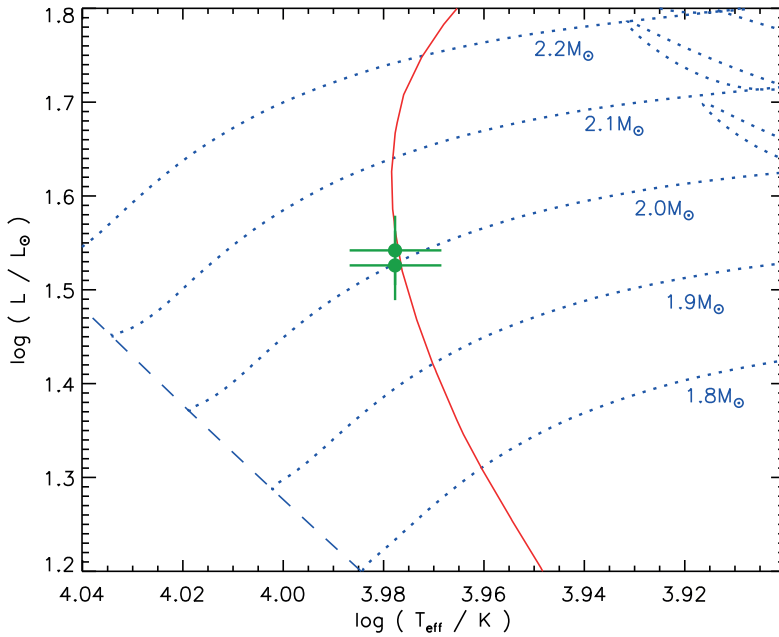


FIG. 5

Hertzsprung–Russell diagram for the components of V596 Pup (filled green circles) and the predictions of the PARSEC 1.2S models⁷¹ for masses of 1.8, 1.9, 2.0, 2.1, and 2.2 M_{\odot} (dotted blue lines with masses labelled) and the zero-age main sequence (dashed blue line), for a metal abundance of $Z = 0.010$. The isochrone for an age of 570 Myr is shown with a solid red line.

borderline consistent with being of the SPB type⁷⁷, with the components of V596 Pup having T_{eff} values at the lower limit of this class⁷⁸.

The orbital frequency of V596 Pup is 0.2176 d^{-1} , and the Loumos & Deeming⁷⁹ frequency resolution is 0.10 d^{-1} . Frequencies f_3 and f_6 are close to being the 157th and 197th multiples of the orbital frequency, but this similarity is of low statistical significance given the frequency resolution of a single *TESS*

TABLE IV

Significant pulsation frequencies found in the TESS sector 61 light curve of V596 Pup after subtraction of the effects of binarity.

Label	Frequency (d^{-1})	Amplitude (mmag)	S/N
f_1	1.9060 ± 0.0010	0.126 ± 0.006	5.0
f_2	30.0686 ± 0.0049	0.027 ± 0.006	5.4
\hat{f}_3	34.1693 ± 0.0019	0.070 ± 0.006	9.2
f_3	38.5870 ± 0.0011	0.125 ± 0.006	11.8
f_5	39.8933 ± 0.0013	0.102 ± 0.006	10.5
\hat{f}_6	42.8533 ± 0.0027	0.049 ± 0.006	6.5
f_7	46.3927 ± 0.0040	0.033 ± 0.006	4.8

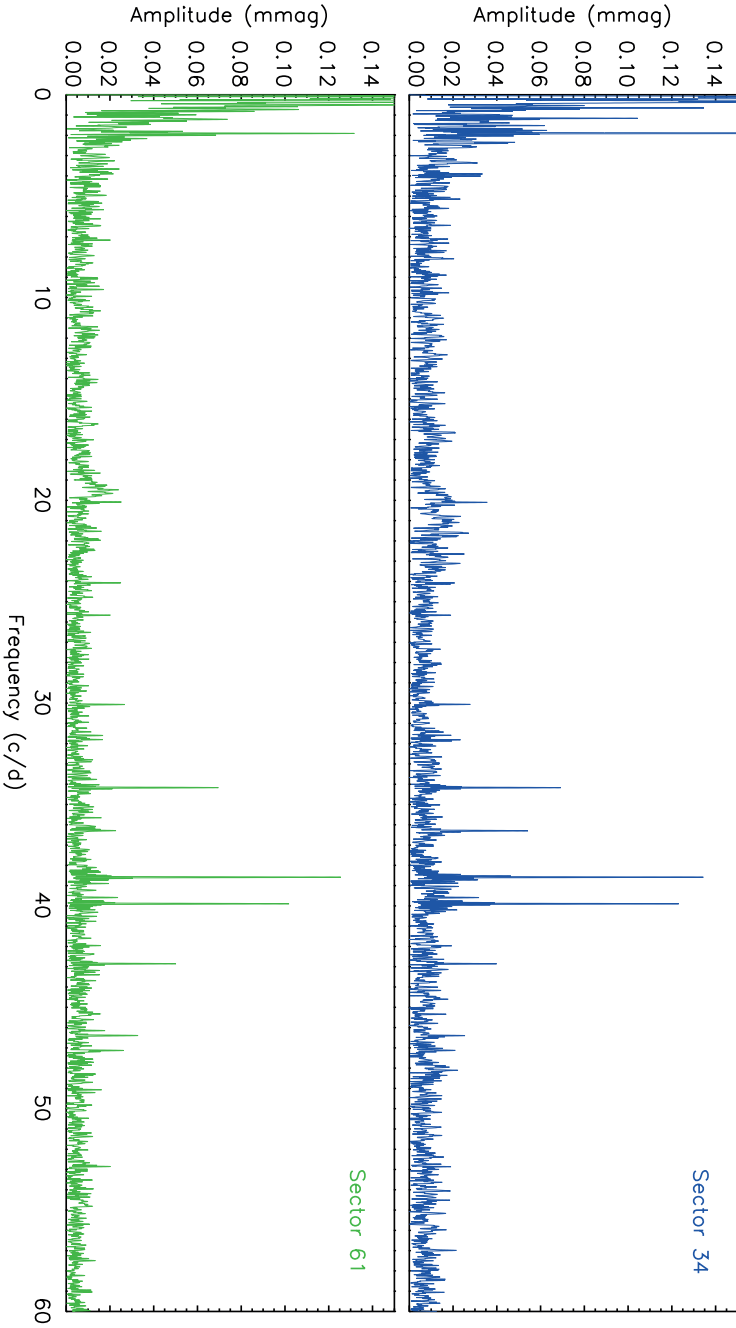


Fig. 6
Frequency spectra of V596 Pup from TESS sector 34 (upper panel, blue lines) and sector 61 (lower panel, green lines).

sector. We are not able to attribute any frequency to an individual star with the available data, and indeed cannot rule out that some or all of the pulsations arise from the close companion.

Summary and conclusions

V596 Pup is a dEB containing two A1V stars in an orbit of period 4.596 d which shows both eccentricity and apsidal motion. We have determined the physical properties of the component stars using two sectors of short-cadence data from *TESS* and published photographic RVs from ACN84. We measure the radii of the stars individually for the first time, rather than the radius of the mean component of the system. The radii are extremely well-determined by the *TESS* data, and are consistent with the spectroscopic light ratio from ACN84. The properties of the system are best matched by theoretical predictions for stars of a metal abundance of $Z = 0.010$ and an age of 570 Myr.

V596 Pup has a companion at 0.4 arcsec which is fainter by 1.7 mag in the *TESS* passband, assuming it is the sole source of third light in the *TESS* data. This companion causes a poor fit to the astrometry in *Gaia* DR3, and thus an uncertain parallax. We instead measure a distance *via* the system's K_s -band apparent magnitude and calibrations of surface brightness *versus* T_{eff} , obtaining 178.4 ± 2.5 pc after correcting for the light from the third star under the assumption that it has the same T_{eff} as the eclipsing stars.

Pulsations are visible in the light-curve of V596 Pup. We subtracted the effects of binarity and measured seven significant pulsation frequencies in the data. Six of these are consistent with p-mode pulsations ($30\text{--}46\text{ d}^{-1}$) and one with g-mode oscillations (1.9 d^{-1}). We assign the higher frequencies to δ Scuti pulsations and the lower frequency to SPB pulsations; the component stars are outside but close to the instability strips for both types of variability. There is a chance that some or all of the pulsations arise from the fainter companion to the binary system.

The current work significantly increases the precision of the radius measurements of the members of the V596 Pup system. Further improvements to the analysis could be obtained by better characterizing the fainter nearby star, obtaining spectroscopic chemical abundances to check our inference of a low metallicity of the system, and measuring its apsidal period precisely to constrain the internal-structure constants of the component stars

Acknowledgements

This paper includes data collected by the *TESS* mission and obtained from the MAST data archive at the Space Telescope Science Institute (STScI). Funding for the *TESS* mission is provided by the NASA's Science Mission Directorate. STScI is operated by the Association of Universities for Research in Astronomy, Inc., under NASA contract NAS 5-26555. This work has made use of data from the European Space Agency (ESA) mission *Gaia*^{*}, processed by the *Gaia* Data Processing and Analysis Consortium (DPAC[†]). Funding for the DPAC has been provided by national institutions, in particular the institutions participating in the *Gaia* Multilateral Agreement. The following resources were used in the course of this work: the NASA Astrophysics Data

*<https://www.cosmos.esa.int/gaia>

†<https://www.cosmos.esa.int/web/gaia/dpac/consortium>

System; the *Simbad* database operated at CDS, Strasbourg, France; and the arXiv scientific-paper preprint service operated by Cornell University.

References

- (1) J. Higl & A. Weiss, *A&A*, **608**, A62, 2017.
- (2) A. Claret & G. Torres, *ApJ*, **859**, 100, 2018.
- (3) A. Tkachenko *et al.*, *A&A*, **637**, A60, 2020.
- (4) C. Aerts, J. Christensen-Dalsgaard & D. W. Kurtz, *Asteroseismology* (Astron. and Astroph. Library, Springer Netherlands, Amsterdam), 2010.
- (5) C. Aerts *et al.*, *Science*, **300**, 1926, 2003.
- (6) M. Briquet *et al.*, *MNRAS*, **381**, 1482, 2007.
- (7) A. García Hernández *et al.*, *A&A*, **559**, A63, 2013.
- (8) T. R. Bedding *et al.*, *Nature*, **581**, 147, 2020.
- (9) K. M. Hambleton *et al.*, *MNRAS*, **434**, 925, 2013.
- (10) C. Maceroni *et al.*, *A&A*, **563**, A59, 2014.
- (11) J. Southworth, S. J. Murphy & K. Pavlovski, *MNRAS*, **520**, L53, 2023.
- (12) Z. Jennings *et al.*, *MNRAS*, **533**, 2705, 2024.
- (13) J. Debosscher *et al.*, *A&A*, **556**, A56, 2013.
- (14) J. Southworth & T. Van Reeth, *MNRAS*, **515**, 2755, 2022.
- (15) J. V. Clausen, *A&A*, **308**, 151, 1996.
- (16) J. Southworth & D. M. Bowman, *MNRAS*, **513**, 3191, 2022.
- (17) J. Southworth *et al.*, *MNRAS*, **497**, L19, 2020.
- (18) J. Southworth, D. M. Bowman & K. Pavlovski, *MNRAS*, **501**, L65, 2021.
- (19) C. I. Eze & G. Handler, *ApJS*, **272**, 25, 2024.
- (20) J. Southworth, *The Observatory*, **141**, 282, 2021.
- (21) J. Southworth, *The Observatory*, **144**, 24, 2024.
- (22) J. Southworth & D. M. Bowman, *The Observatory*, **142**, 161, 2022.
- (23) J. Southworth, *The Observatory*, **143**, 254, 2023.
- (24) E. Høg *et al.*, *A&A*, **355**, L27, 2000.
- (25) R. M. Cutri *et al.*, *2MASS All Sky Catalogue of Point Sources*, NASA/IPAC Infrared Science Archive, Caltech, US), 2003.
- (26) Gaia Collaboration, *A&A*, **674**, A1, 2023.
- (27) D. Hoffleit & C. Jaschek, *The Bright Star Catalogue* (Yale University Observatory, 1991, 5th ed.), 1991.
- (28) A. J. Cannon & E. C. Pickering, *Annals of Harvard College Observatory*, **93**, 1, 1919.
- (29) Gaia Collaboration, *A&A*, **649**, A1, 2021.
- (30) K. G. Stassun *et al.*, *AJ*, **158**, 138, 2019.
- (31) J. Andersen, J. V. Clausen & B. Nordström, *A&A*, **134**, 147, 1984.
- (32) W. Strohmeier, R. Knigge & H. Ott, *IBVS*, **100**, 1, 1965.
- (33) J. Andersen & B. Nordström, *A&AS*, **29**, 309, 1977.
- (34) E. H. Olsen, *A&AS*, **29**, 313, 1977.
- (35) P. N. Kholopov *et al.*, *IBVS*, **1921**, 1, 1981.
- (36) J. V. Clausen & B. Nordström, *A&A*, **83**, 339, 1980.
- (37) B. Grønbech, E. H. Olsen & B. Strömberg, *A&AS*, **26**, 155, 1976.
- (38) R. R. Shobbrook, *Journal of Astronomical Data*, **10**, 1, 2004.
- (39) N. N. Samus *et al.*, *Astronomy Letters*, **32**, 263, 2006.
- (40) E. V. Kazarovets *et al.*, *IBVS*, **5721**, 1, 2006.
- (41) H. M. Jeffers, W. H. van den Bos & F. M. Greeby, *Index Catalogue of Visual Double Stars, 1961.0*, 1963.
- (42) H. A. McAlister *et al.*, *AJ*, **93**, 688, 1987.
- (43) H. A. McAlister, W. I. Hartkopf & O. G. Franz, *AJ*, **99**, 965, 1990.
- (44) Z. Penoyre, V. Belokurov & N. W. Evans, *MNRAS*, **513**, 5270, 2022.
- (45) A. Castro-Ginard *et al.*, *A&A*, **688**, A1, 2024.
- (46) A. Giménez, *ApJ*, **297**, 405, 1985.
- (47) A. Claret, *A&A*, **327**, 11, 1997.
- (48) A. V. Petrova & V. V. Orlov, *Astrophysics*, **45**, 334, 2002.
- (49) A. Claret & B. Willems, *A&A*, **388**, 518, 2002.
- (50) M. Wolf *et al.*, *A&A*, **509**, A18, 2010.
- (51) A. Claret *et al.*, *A&A*, **654**, A17, 2021.
- (52) F. Kahraman Aliçavuş *et al.*, *MNRAS*, **524**, 619, 2023.
- (53) G. R. Ricker *et al.*, *Journal of Astronomical Telescopes, Instruments, and Systems*, **1**, 014003, 2015.
- (54) Lightkurve Collaboration, 'Lightkurve: Kepler and TESS time series analysis in Python', Astrophysics Source Code Library, 2018.

- (55) J. M. Jenkins *et al.*, in *Proc. SPIE*, 2016, *Society of Photo-Optical Instrumentation Engineers Conference Series*, vol. **9913**, p. 99133E.
- (56) C. X. Huang *et al.*, *RNAAS*, **4**, 204, 2020.
- (57) J. Southworth, P. F. L. Maxted & B. Smalley, *MNRAS*, **351**, 1277, 2004.
- (58) J. Southworth, *A&A*, **557**, A119, 2013.
- (59) D. Hestroffer, *A&A*, **327**, 199, 1997.
- (60) P. F. L. Maxted, *A&A*, **616**, A39, 2018.
- (61) J. Southworth, *The Observatory*, **143**, 71, 2023.
- (62) A. Claret & J. Southworth, *A&A*, **664**, A128, 2022.
- (63) A. Claret & J. Southworth, *A&A*, **674**, A63, 2023.
- (64) J. Southworth, *The Observatory*, **141**, 234, 2021.
- (65) A. Prša *et al.*, *AJ*, **152**, 41, 2016.
- (66) J. Southworth, P. F. L. Maxted & B. Smalley, *A&A*, **429**, 645, 2005.
- (67) J. Zorec & F. Royer, *A&A*, **537**, A120, 2012.
- (68) P. Kervella *et al.*, *A&A*, **426**, 297, 2004.
- (69) J. M. Carpenter, *AJ*, **121**, 2851, 2001.
- (70) L. Girardi *et al.*, *A&A*, **391**, 195, 2002.
- (71) Y. Chen *et al.*, *MNRAS*, **444**, 2525, 2014.
- (72) A. Bressan *et al.*, *MNRAS*, **427**, 127, 2012.
- (73) P. Lenz & M. Breger, *Communications in Asteroseismology*, **146**, 53, 2005.
- (74) M. Breger, in *Delta Scuti and Related Stars* (M. Breger & M. Montgomery, ed.), 2000, *Astronomical Society of the Pacific Conference Series*, vol. 210, pp. 3–42.
- (75) R. Kuschnig *et al.*, *A&A*, **328**, 544, 1997.
- (76) S. J. Murphy *et al.*, *MNRAS*, **485**, 2380, 2019.
- (77) C. Waelkens, *A&A*, **246**, 453, 1991.
- (78) X.-d. Shi *et al.*, *ApJS*, **268**, 16, 2023.
- (79) G. L. Loumos & T. J. Deeming, *Ap&SS*, **56**, 285, 1978.

CORRESPONDENCE

*To the Editors of 'The Observatory'
Exquisite Precision*

In a recent book review¹, in reference to one of the échelle spectrographs with a precision of 10 cm s⁻¹ on the ESO *Very Large Telescope*, Tatum wondered "... whether astronomers can really make use of such exquisite precision". There are at least two fields of study where the answer is 'yes'. One involves the detection of exoplanets *via* the changing radial velocity of a parent star. The change in the radial velocity of the Sun due to the Earth is about 10 cm s⁻¹. Thus, even higher resolution would be needed in order to detect less massive and/or more distant planets around Sun-like stars, and even more if the system is not seen edge-on. The same goes for a more massive star, and moreover in such a case a planet in the habitable zone would be further away as well, reducing the change in radial velocity even more.

The other, at the other end of the astronomical scale, is cosmology. The cosmological redshift z is given by $R_0/R - 1$, where R_0 is the scale factor now and R the scale factor at the time of emission. One usually assumes that R_0 is constant, since time-scales directly familiar to humans are orders of magnitude shorter than the light-travel time from an object with a significant cosmological